



Aalborg Universitet

AALBORG UNIVERSITY
DENMARK

Method for Predicting Void Ratio and Triaxial Friction Angle from Laboratory CPT at Shallow Depths

Larsen, Kim André; Ibsen, Lars Bo

Publication date:
2006

Document Version
Publisher's PDF, also known as Version of record

[Link to publication from Aalborg University](#)

Citation for published version (APA):
Larsen, K. A., & Ibsen, L. B. (2006). *Method for Predicting Void Ratio and Triaxial Friction Angle from Laboratory CPT at Shallow Depths*. Department of Civil Engineering, Aalborg University. AAU Geotechnical Engineering Papers No. R0608

General rights

Copyright and moral rights for the publications made accessible in the public portal are retained by the authors and/or other copyright owners and it is a condition of accessing publications that users recognise and abide by the legal requirements associated with these rights.

- Users may download and print one copy of any publication from the public portal for the purpose of private study or research.
- You may not further distribute the material or use it for any profit-making activity or commercial gain
- You may freely distribute the URL identifying the publication in the public portal -

Take down policy

If you believe that this document breaches copyright please contact us at vbn@aub.aau.dk providing details, and we will remove access to the work immediately and investigate your claim.

GEOTECHNICAL ENGINEERING
DEPARTMENT OF CIVIL ENGINEERING
AALBORG UNIVERSITY

Appendix A.

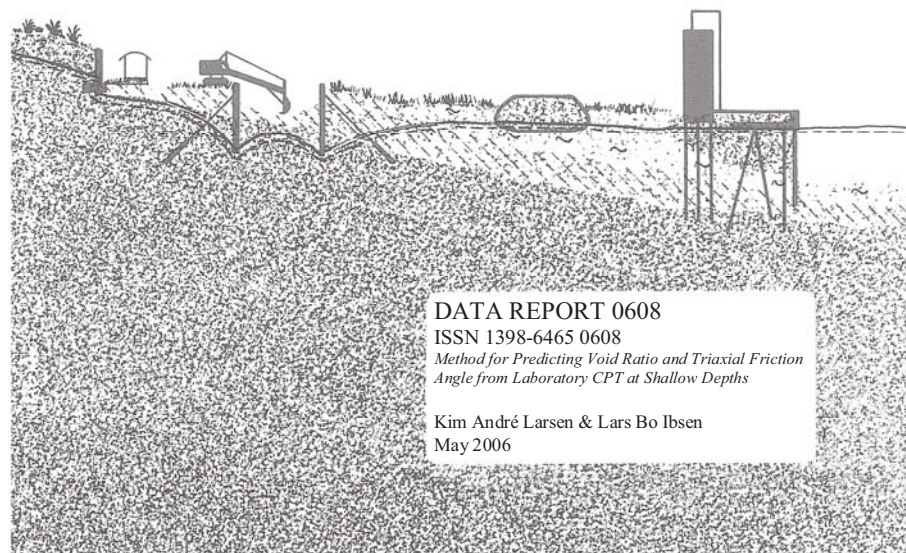


Table of content

1	Introduction	3
2	Laboratory Cone Penetration Testing Probe.....	4
2.1	Construction of the Laboratory Cone Penetration Probe.....	4
2.2	Tests with the laboratory CPT-probe	5
3	Aalborg University Sand No. 0	9
3.1	Description of Aalborg University Sand No.0.....	9
3.2	Behaviour of Aalborg University Sand No.0.....	10
4	Interpretation of CPT	14
4.1	Presentation of selected method from the literature.....	14
4.1.1	Janbu and Senneset (1975).....	15
4.1.2	Lunne and Christoffersen (1983).....	15
4.1.3	Bolton and Lau (1993).....	16
4.2	Comparison of methods from literature with test results.....	17
4.3	Calibration of CPT-test for shallow depths	18
5	Conclusion	22
6	References	23
7	Appendix I: Results from tests.	25
8	Appendix II: Evaluation of tests.	37

1 Introduction

In this report an investigation of the relationship between the tip resistance, q_c of a laboratory CPT-probe versus the relative density, D_r and friction angle, ϕ of Aalborg University Sand No. 0 is carried out. A method for estimating the relative density and the triaxial friction angle from the cone resistance of the laboratory probe is proposed.

The suggested method deals with the fact that the friction angle is depended of the stress level especially at low stresses. The method includes a calibration of the cone resistance from the laboratory CPT at shallow depths i.e. low values of d/D against the properties of Aalborg University sand No. 0.

2 Laboratory Cone Penetration Testing Probe

In connection with a Ph.D-study on CPT-testing, a small scale CPT-probe was manufactured at the geotechnical laboratory at Aalborg University, Luke (1994). The probe was manufactured with a length of the shaft at 400mm, but due to the need for investigations in greater depths the probe is modified regarding the shaft length. A presentation of the new probe is given below.

2.1 Construction of the Laboratory Cone Penetration Probe

The laboratory CPT-probe is only capable of determining the tip resistance in contrary to the probes used in the field. These probes are also capable of determining the pore pressure and the sleeve friction during penetration. An illustration of the modified laboratory CPT- probe is shown in Figure 2.1

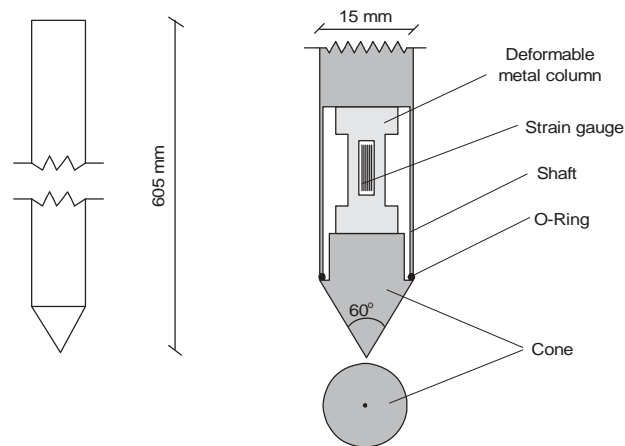


Figure 2.1 Illustration of the modified laboratory cone penetration probe.

The new laboratory CPT-probe has the following geometrical measures:

- Penetration length: 605 mm
- Cone diameter: 15 mm
- Cone area: 176,7 mm²
- Cone angle: 60°

Appendix A

The diameter of the laboratory CPT-probe was originally predetermined to 15mm to avoid influence from the calibration chamber used, Luke (1994).

A deformable metal column and four strain gauges constitute the load cell in the probe as shown on Figure 2.1. The four strain gauges work as two active and two passive gauges. The two active gauges are attached to the deformable metal column vertically and the two passive is attached horizontally. The strain gauges are coupled in a full-bridge connection as shown in Figure 2.2.

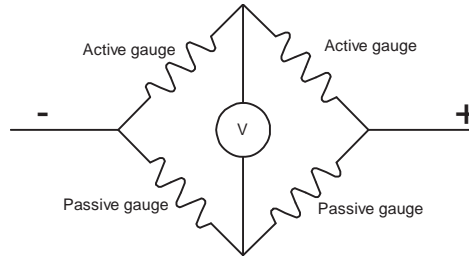


Figure 2.2 Full-bridge connection for the load cell in the CPT-probe.

During the penetration tests the cone resistance, q_c and the penetration depth, d are measured using a computer. The displacement transducer and the strain gauges are connected to the computer through a “spider 8” sampling device.

The constructed load cell is calibrated by use of a calibration bench where the tip is loaded with a known external force in the direction of the probe. The laboratory CPT-probe is found to have a maximum loading capacity of 1200N.

2.2 Tests with the laboratory CPT-probe

Several penetration tests are performed using a cylindrical test box (calibration chamber) and a larger test box, developed for small scale testing of foundations. The construction of the large test box and the procedure for preparation of the sand in this test box is described in Larsen & Ibsen (2006). The large test box is shown in Figure 2.3. All tests in connection with this report are carried out in water saturated sand.

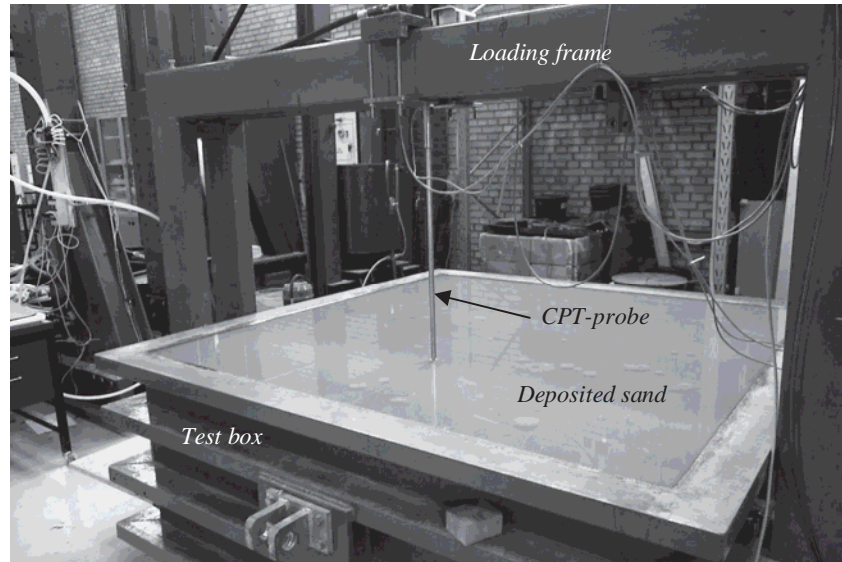


Figure 2.3 The large test box used for the tests with the laboratory CPT-probe. The probe is seen in the middle of the picture ready for penetration.

The calibration chamber is constructed in a way similar to the test box. The inner diameter of the calibration chamber is 525mm and the inner depth is 600mm. The calibration chamber is illustrated in Figure 2.4.

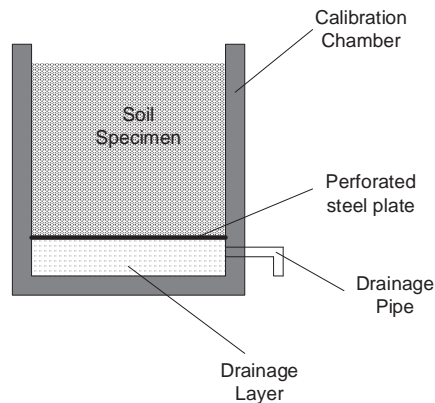


Figure 2.4 Illustration of calibration chamber.

The calibration container consists of a thick steel cylinder with a corresponding steel plate welded at the lower end as bottom. A drainage layer consisting of small stones is used for distributing the water before entering the soil sample above. Between the drainage layer and the soil sample a perforated steel plate is placed to prevent the sand from entering the drainage layer. The water is led in and out of the calibration chamber through a drainage pipe in the side of the chamber, through the drainage layer.

Appendix A

In order to vary the void ratios of the soil samples, different compactness methods are used throughout the study. The location of samples extracted and CPT's performed etc. is defined according to Figure 2.5.

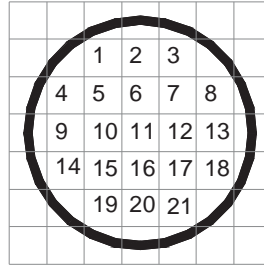


Figure 2.5 Discretization of the soil surface in the calibration container.

The following preparation procedures are used to compact the soil sample during the test program:

- Water pluviation. The sand is deposited with a very large void ratio by dropping the sand through water. This method gives a small relative density.
- Compactness using a rod vibrator. The sand is compacted by vibrating saturated sand with a rod vibrator. The method is described in Larsen & Ibsen (2006) for the large test box. This method gives a large relative density.
- Compactness of the sand by vibrating the container externally with a hydraulic hammer located on the side of the calibration chamber. This method gives intermediate values of the relative density.

The cone penetration tests in the laboratory are performed with a penetration rate of 5 mm/s, with the use of a hydraulic cylinder, see Figure 2.6. The standard CPT's in the field are normally carried out with a penetration rate of 20 mm/s.

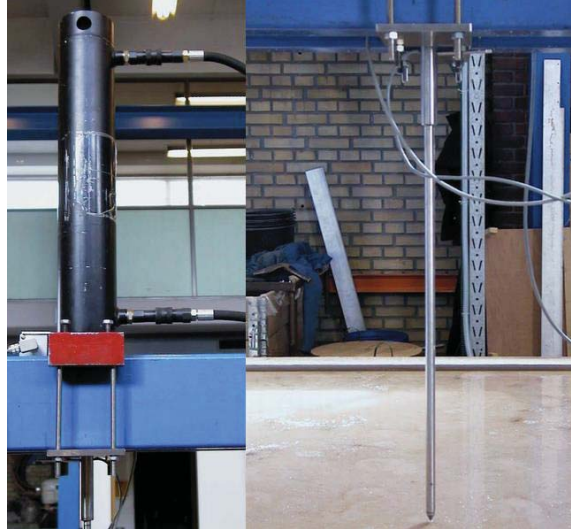


Figure 2.6 Left: Hydraulic cylinder used to penetrate the probe with a constant penetration rate. Right: Laboratory CPT-probe ready for penetration

After each test with the laboratory CPT-probe the void ratio is measured by extracting samples with known volume in different depths. The void ratio is measured from each sample by weighing and drying the soil.

The results from the test series are presented in the data sheets in appendix I. The preparation procedure and the location of CPT and samples for each set of experiment are given in the data sheets. In total 12 set of experiments is executed in sand samples prepared with the above mentioned methods and a combination of these.

3 Aalborg University Sand No. 0

The sand used in the experiments is Aalborg University Sand No. 0 (Baskarp Sand No. 15). Results from several triaxial tests are summarized in the following to determine the behaviour of the sand. A description of the sand is given below.

3.1 Description of Aalborg University Sand No.0

Aalborg University Sand No. 0 is a graded sand from Sweden. The shape of the largest grains is round while the small grains have sharp edges. The main part of Aalborg University Sand No. 0 is quartz, but it also contains feldspar and biotite.

The properties of Aalborg Universitet Sand No.0 are well-known because of available results from triaxial, cubical and other tests. All tests are performed in the laboratory at Aalborg University. Information's from triaxial tests are used to correlate the response of the tests with the laboratory CPT-probe to the relative density and strength of the sand.

For classification of the sand the performed tests are:

- Sieve test
- Grain density, d_s
- Maximum, e_{\max} and minimum, e_{\min} void ratio

From the sieve test the following parameters have been determined:

- $d_{50} = 0.14 \text{ mm}$
- $d_{60}/d_{10} = U = 1.78$

The distribution of the grains is illustrated in Figure 3.1.

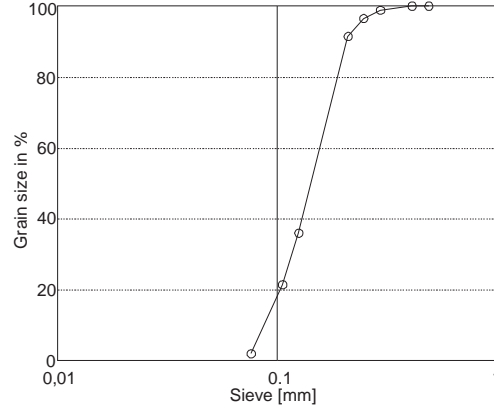


Figure 3.1 Distribution of grains for Aalborg University Sand No. 0.

The grain density, maximum and minimum void ratios have been determined to:

- $d_s = 2.64$
- $e_{\max} = 0.858$
- $e_{\min} = 0.549$

All the tests have been performed according to the standard procedures used in the laboratory, DGF-Bulletin (2001).

3.2 Behaviour of Aalborg University Sand No.0.

Since the void ratio is known with depth for each CPT the correlation between the void ratio and the friction angle can be investigated. The friction angle is throughout the report determined as the effective secant friction angle, φ'_s from a triaxial test by the following equation:

$$\sin(\varphi'_s) = \frac{\sigma'_1 - \sigma'_3}{\sigma'_1 + \sigma'_3} \quad (3.1)$$

where σ'_1 and σ'_3 is the major and minor effective principal stress at failure.

The following results are derived from previous performed triaxial tests on Aalborg University Sand No. 0 with different void ratios and different confining pressures, Ibsen & Bødker (1994), Borup & Hedegaard (1995), Ibsen et al. (1995) and Andersen et al. (1998).

The influence from the minor effective principal stress, σ'_3 on the strength of the sand is investigated using the results from the above mentioned triaxial experiments. A description of this influence has been proposed by Jacobsen (1970) by the following equation.

Appendix A

$$q' = \sigma'_1 - \sigma'_3 = \frac{\sin(\varphi'_{t,a})}{1 - \sin(\varphi'_{t,a})} \sigma'_3 \left(1 + \frac{c'_{t,a} \cdot \cot(\varphi'_{t,a})}{m \cdot \sigma'_3} \right)^m \quad (3.2)$$

where q' is the deviatoric stress and c' is the effective cohesion. The index t and a denotes that the parameter is the tangent parameter at high stresses (asymptote) and m is a parameter that describes the curvature of the failure envelope at low stress levels.

The enveloping surface given by equation (3.2) is fitted to the result from the triaxial tests. For void ratios of 0.61, 0.7 and 0.85 the calibration are performed by Didriksen and Kristensen, (2000). The fitted parameters are listed in Table 3.1.

Table 3.1 Fitted strength parameters for Aalborg University Sand No.0.

Void ratio, e	$\varphi'_{t,a}$ [°]	$c'_{t,a}$ [kPa]	m
0,55	41,00	19,90	0,350
0,61	38,60	34,57	0,197
0,70	34,21	40,42	0,187
0,85	30,93	7,00	0,451

The failure envelopes according the fitted strength parameters in Table 3.1 can be seen in Figure 3.2 where the stress situations at failure for the performed triaxial tests are plotted as well.

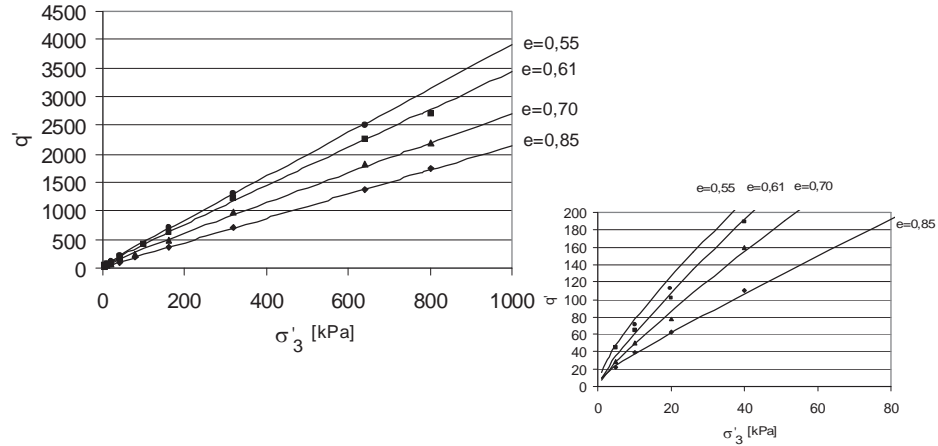


Figure 3.2 Failure envelopes from triaxial tests on Aalborg University Sand No.0. The line represents the fitted envelopes and the markers represent failure values from performed triaxial tests.

The variation of the triaxial secant friction angle with respect to the minor principal stress, σ'_3 can be calculated when equation (3.1) is transcribed into a function of σ'_3 and the deviatoric stress, q' according to equation (3.2):

$$\sin(\varphi'_s) = \frac{q'}{2 \cdot \sigma'_3 + q'}$$

or

$$\sin(\varphi'_s) = \frac{\frac{\sin(\varphi'_{t,a})}{1 - \sin(\varphi'_{t,a})} \sigma'_3 \left(1 + \frac{c'_{t,a} \cdot \cot(\varphi'_{t,a})}{m \cdot \sigma'_3} \right)^m}{2 \cdot \sigma'_3 + \frac{\sin(\varphi'_{t,a})}{1 - \sin(\varphi'_{t,a})} \sigma'_3 \left(1 + \frac{c'_{t,a} \cdot \cot(\varphi'_{t,a})}{m \cdot \sigma'_3} \right)^m} \quad (3.3)$$

The fitted variation of the triaxial secant friction angle for different void ratios after equation (3.3) are shown in *Figure 3.3*

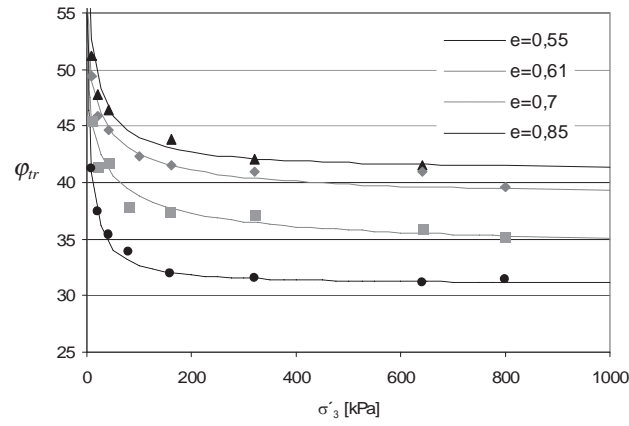


Figure 3.3 Variation of the triaxial secant friction angle with the minimal stress at failure after equation (3.3). The results from the triaxial tests are shown as marks.

The triaxial secant friction angle is from Figure 3.3 seen to depend on both the stress level as well as the void ratio. The relation between the void ratio and the friction angle can be described using Kerisel's formula.

$$e \cdot \tan(\varphi) = C \quad (3.4)$$

where C is a constant which for sand usually is between 0.4 and 0.5. In Figure 3.4 the constant in Kerisel's formula is fitted to the triaxial results at different stress levels i.e. the confining pressure. The constants are fitted according to the failure envelopes from equation (3.2). Selected failure values from these envelopes are shown in the figure as well.

Appendix A

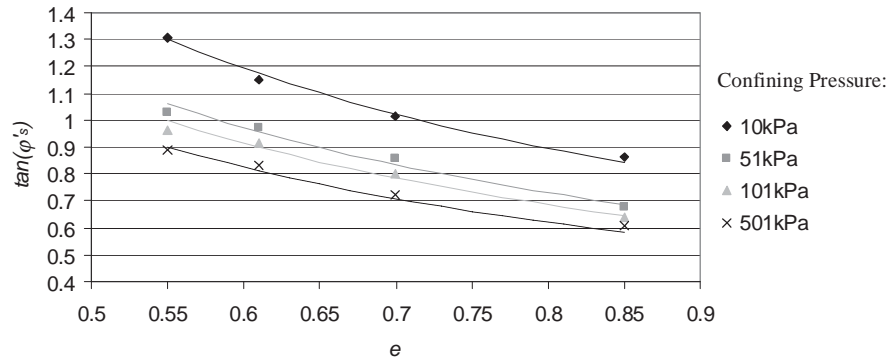


Figure 3.4 Relationship between the void ratio and $\tan(\phi_s)$ from equation (3.2) (grey scale marks) at different confining pressures. The relationship suggested by Kerisel is shown for the respective stress levels by lines.

From Figure 3.4 it can be seen that the relationship proposed by Kerisel fits the results from the triaxial tests very well. Though it is found that the constant in equation (3.4) varies with the stress level. The value of the constant C as a function of the minor principal stress is shown in Figure 3.5.

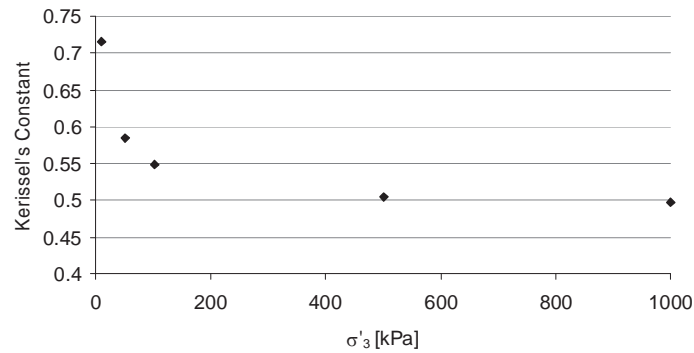


Figure 3.5 Variation of Kerisel's constant with respect to the minor principal stress.

The constant in Kerisel's formula is seen to decrease with increasing stress level, until reaching a constant value of $C = 0.496$ at large stresses.

4 Interpretation of CPT

The resistance against penetration of the CPT-probe into the sand depends on several factors. Some of these factors are the geometry and material of the probe. The geometrical factors are the angle of the wedge on the cone, the diameter of the probe and the material property are reflected by the roughness of the cone. Furthermore the conditions of the soil are reflected in the penetration resistance. This is the density, the friction angle, the compressibility and the stress conditions in the soil. Besides this the degree of saturation, the size of the grain particles as well as the relative penetration depth and penetration rate is of importance.

4.1 Presentation of selected method from the literature

Different methods of predicting the strength parameters of soils from cone penetration tests are proposed in the literature. Some of these suggestions are presented in the following, and will be investigated for their usefulness in the prediction of the friction angle from the laboratory CPT's.

Methods used to calculate the cone resistance of the cone probe, $q_c = Q/A$ presented in this report are all based on the classical bearing capacity formula by, Terzaghi (1943):

$$\frac{Q}{A} = \frac{1}{2} \gamma' B N_\gamma + q' N_q + c' N_c \quad (4.1)$$

where γ' is the effective unit weight of the soil, B is the width of the foundation, q is the overburden pressure and N_γ , N_q and N_c are bearing capacity factors. The bearing formulation in equation (4.1) assumes that the bearing capacity can be divided into three terms. The first term is the bearing capacity of a surface foundations resting on a cohesion-less soil. The second term is the bearing capacity from the overburden pressure and the last term is the bearing capacity from the cohesion in the soil. Equation (4.1) can for a friction or cohesion-less material be reduced to:

$$\frac{Q}{A} = \frac{1}{2} \gamma' B N_\gamma + q' N_q \quad (4.2)$$

The last term (q -term) in equation (4.2) can be shown to dominate as the CPT is penetrated into the soil. Thus γ -term is often ignored, and the relation between the tip resistance of the CPT and the bearing capacity factor N_q is merely expressed by:

$$N_q = \frac{q_c}{\sigma_v} \quad (4.3)$$

Appendix A

where N_q , for a pure friction material, is given by the cone resistance divided by the effective stresses at rest in the depth equal to the position of the cone.

Selected correlations between the bearing capacity factor N_q and the friction angle relevant for CPT's from the literature are presented in the following sections.

4.1.1 Janbu and Senneset (1975)

Janbu and Senneset (1975) suggested an expression for the bearing capacity factor N_q , determined from the stress field illustrated in Figure 4.1. The expression are evaluated assuming plain strain conditions. Thus the plane friction angle must be used along with an appropriate shape-factor on N_q .

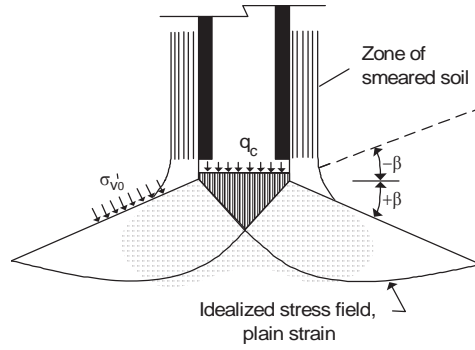


Figure 4.1 Idealized stress field used to determine N_q after Janbu & Senneset (1975)

The evaluated expression of N_q from the stress field in Figure 4.1 is given as follows:

$$N_q = \tan^2\left(\frac{\pi}{4} + \frac{1}{2}\varphi\right) \cdot e^{(\pi - 2\beta)\tan(\varphi)} \quad (4.4)$$

Where β is the angle of plastification in the idealized stress field geometry shown in Figure 4.1. The value of β for sand is usually between 15° and -15° . The value of β is observed to change with the angle of internal friction, which must be taken into account.

4.1.2 Lunne and Christoffersen (1983)

Lunne and Christoffersen (1983) suggested a modified version of the expression by Janbu and Senneset (1975) presented above, and is given as follows.

$$N_q = \tan^2\left(\frac{\pi}{4} + \frac{1}{2}\varphi\right) \cdot e^{(\frac{\pi}{3} + 4\varphi)\tan(\varphi)} \quad (4.5)$$

Equation (4.5) is modified in order to describe the variation of β with the change of φ .

4.1.3 Bolton and Lau (1993)

A set of bearing capacity factors for strip and circular footings is evaluated by Bolton and Lau (1993). The values derived for circular footings with smooth base are given in Table 4.1 These values is determined from an axis-symmetric stress situation, thus the factors includes shape factors and is a function of the triaxial friction angle. The width of the foundation in equation (4.1) and (4.2) is equal to the diameter of the cpt-probe if these values are used.

Table 4.1 Bearing capacity factors for circular smooth footings, after Bolton and Lau (1993).

φ [o]	N_q	N_γ
	Smooth or rough base	Smooth base
5	1.65	0.06
10	2.80	0.21
15	4.70	0.60
20	8.30	1.30
25	15.2	3.00
30	29.5	7.10
31	34	8.60
32	39	10.3
33	45	12.4
34	52.2	15.2
35	61	18.2
36	71	22
37	83	27
38	99	33
39	116	40
40	140	51
41	166	62
42	200	78
43	241	99
44	295	125
45	359	160
46	444	210
47	550	272
48	686	353
49	864	476
50	1103	621
51	1427	876
52	1854	1207

The values in Table 4.1 are evaluated assuming a flat base of the foundation, i.e. a wedge angle =180 degrees.

4.2 Comparison of methods from literature with test results.

The values of the bearing capacity N_q presented in section 4.1 are compared in Figure 4.2.

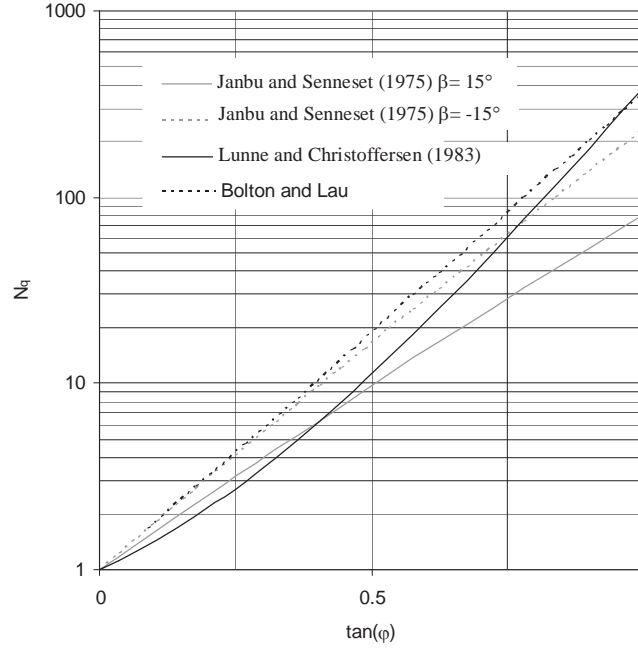


Figure 4.2 Comparison of the bearing capacity factors, N_q .

The values of N_q in Figure 4.2 are evaluated assuming associated flow. Sand is known to exhibit a behaviour that is non-associated. Thus a reduced friction angle, ϕ_d should be used to estimate the value of N_q . A relation that accounts for this is given by the following relation, Jakobsen (1989).

$$\tan(\phi'_d) = \frac{\sin \phi'_r \cos \psi}{1 - \sin \phi'_r \sin \psi} \quad (4.6)$$

where ψ is the dilation angle of the sand.

The friction angle is in chapter 3 shown to vary extensively with the stress levels at a low stress level. The friction angle that corresponds to the measured cone resistance is unknown during penetration of the CPT-probe due to the variation with stresses. The friction angle at large stress levels is however unique for a given compactness of the soil sample. In appendix II this friction angle is used to compare the measured cone resistance with the proposed values of N_q in Figure 4.2. The friction angle used is the reduced friction angle according to equation (4.6) assuming $\psi = \phi_r - 30^\circ$.

The results clearly shows that this friction angle gives a penetration resistance that is too low compared with the measured resistance. The variation of N_q proposed by Bolton & Lau (1993) is in appendix II used to estimate the reduced as well as the triaxial friction angle from the measured cone resistance. This friction angle is seen to be significantly higher then the measured triaxial friction angle determined at large stresses, also presented in appendix II. Thus the stress level in the soil during penetration of the CPT-probe is lower than the stress level that entails a constant value.

The mean stress level in the soil affected by the penetration of the CPT-probe is not known. Hence the estimated friction angle from e.g. Bolton and Lau (1993) is not useful for characterizing the soil tested.

4.3 Calibration of CPT-test for shallow depths

The stress levels present in the laboratory during small scale testing of geotechnical problems are extremely small compared to true scale. Thus the friction angle must be determined at a corresponding stress level. The friction angle determined from the above presented methods corresponds to a stress level that often is different from e.g. a loading test on a surface foundation. Hence this is not useful in evaluating the measured results

Because of this a method for determining the triaxial friction angle at a known stress level for CPT-tests at shallow depths is suggested and calibrated against Aalborg University Sand No.0. As shown in section 3 the influence of stress level on the friction angle is different for different void ratios. At large stresses a unique relation between the void ratio and the friction according to Kerisel's formula was observed. This relation is used to propose a method that is based on equation (4.3) using a bearing capacity factor N_q^* . The bearing capacity factor N_q^* is calibrated against the triaxial friction angle at large stresses according to the following definition:

$$N_q^* = N_q \cdot d_q \quad (4.7)$$

where N_q is the bearing capacity suggested by Bolton & Lau (1993) for a circular and smooth footing and d_q is a depth factor that takes into account the effect of the penetration depth i.e. the stress level on the friction angle. The bearing capacity factor is a function of the triaxial friction angle and is shown in Figure 4.3.

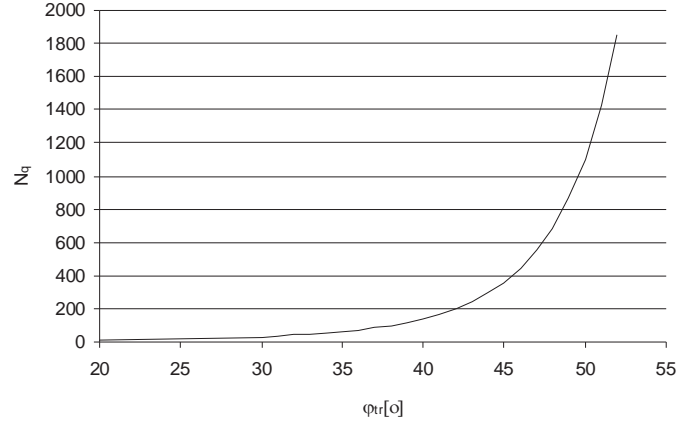


Figure 4.3 Bearing capacity factor for smooth circular footings after Bolton & Lau (1993).

The depth factor is from the tests in Appendix I found to be a function of the friction angle and the penetration depth according to the following relation:

$$d_q = 1 + \alpha(\varphi) \cdot \frac{d}{D} \quad (4.8)$$

The value of α in equation (4.8) has been investigated by back calculation of the cone resistance from the tests with the laboratory CPT-probe. From the measured void ratios the corresponding triaxial friction angles at high stresses are determined from equation (3.4). The variation of α has been found to follow:

$$\alpha = 3 \cdot 10^{-16} \cdot \varphi^{9.4176} \quad (4.9)$$

The variation of α is shown in Figure 4.4. The value of α is seen to increase with increasing friction angle. The back calculated values from the laboratory CPT's are shown in the figure as well. The fitted expression of α is seen from the figure to capture the variation well with exception of a few outliers. The outliers are identified to originate from measurements at low penetration depths.

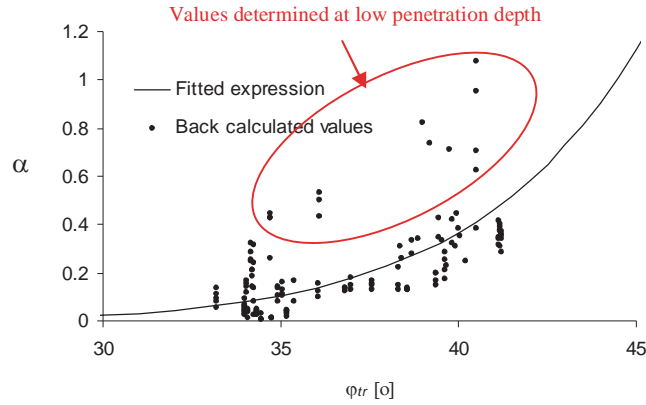


Figure 4.4 Variation of α with the triaxial friction angle at large stress levels.

The proposed method is in appendix II compared with the tests carried out. The method is from comparison with measured results shown capable of predicting the void ratio and friction angle at large stress levels as well as the cone resistance.

From the comparisons carried out in appendix II, it is seen that for penetration depth below 100mm the proposed method generally overestimates the friction angle and there by underestimates the void ratio.

The cone resistance from the laboratory CPT-probe has been calibrated against the triaxial friction angle at large stresses. From this the void ratio and the stress dependency of the friction angle can be determined according to Figure 4.5, cf. section 3.2.

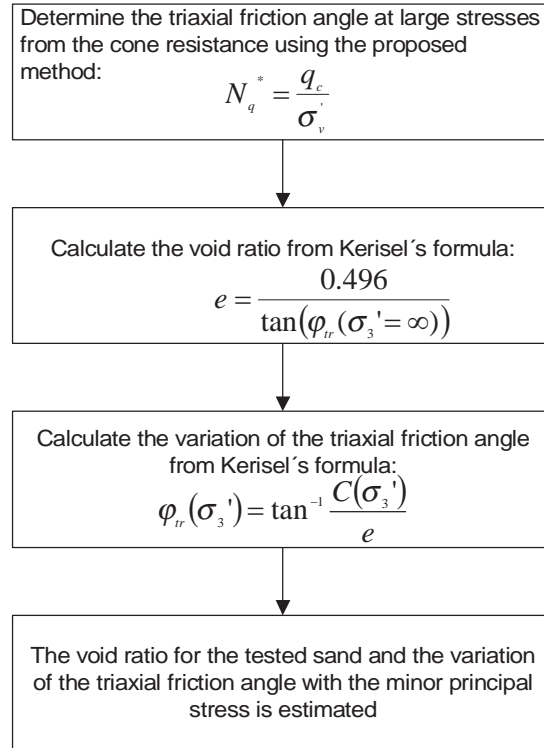


Figure 4.5 Proposed evaluation procedure for determining the void ratio and the triaxial friction angle from a test with the laboratory CPT-probe in Aalborg University Sand No. 0 at shallow depth.

5 Conclusion

A method to estimate the void ratio and the triaxial friction angle from the cone resistance using a laboratory CPT-cone in Aalborg University Sand No. 0 is proposed.

The method is based on Terzaghi's bearing capacity formula using the values of the bearing capacity factors given by Bolton & Lau (1993) for circular and smooth footings including a depth factor. The depth factor is calibrated from the results of 12 test series with the laboratory probe.

The proposed method is based on the triaxial friction angle at large stresses since Kerisel's relationship in this case gives a unique result. From this friction angle the method can be used to estimate the complete variation of the triaxial friction angle with the stress level for the tested sand.

6 References

- Andersen, A.T. ; Madsen, E.B & Schaarup-Jensen, A.L. (1998)
Data Report 9701, Eastern Scheldt Sand, Baskarp Sand No. 15
Geotechnical Engineering Group, Aalborg University
- Bolton & Lau (1993)
Vertical bearing capacity factors for circular and strip footings on Mohr-Coulomb soil
Canadian Geotechnical Journal 30. (1993)
- Borup, M. & Hedegaard, J. (1995)
Data Report 9403, Baskarp Sand No. 15
Geotechnical Engineering Group, Aalborg University
- Det Norske Veritas, (1992) [DNV (1992)]
Foundations, Classification Notes No. 30.4
Det Norske Veritas, Norway.
- Didriksen, L.R. and Kristensen, J. (2000)
Konceptvurdering af bøttefundament til en offshorevindmølle.
M.sc.-thesis. Aalborg University. In Danish.
- Ibsen, L.B. ; Borup, M. & Hedegaard, J. (1995)
Data Report 9501, Triaxial Tests on Baskarp Sand No. 15
AAU Geotechnical Engineering Papers ISSN 1398-6465 R9501
Geotechnical Engineering Group, Aalborg University
- Ibsen, L.B. & Bødker, L. (1994)
Data Report 9301, Baskarp Sand No. 15
Geotechnical Engineering Group, Aalborg University
- Jacobsen M. (1970)
New oedometer and New Triaxial apparatus for firm soil. DGI
Bulletin No. 27 Danish geotechnical society.
- Jacobsen, M. (1989)
Lærebog i videregående geoteknik I "Brud i jord".
Aalborg Universitet In danish

- Larsen, K.A. & Ibsen, L.B. (2006)
Data Report 0201, Bucket foundations on Aalborg University Sand No. 0.
ISSN 1398-6465 R0201. Department of civil engineering, Aalborg University Version 4 May 2006
- Luke, K. (1994)
The use of CPT in Danish soils with special emphasis on measuring the undrained shear strength.
Ph.D. Thesis ATV Project EF 368, Aalborg University
- Lunne and Christoffersen., (1983)
Interpretation of Cone Penetrometer Data for Offshore Sands
Offshore Technology Conference OTC 4464
- Terzaghi K. (1943)
Theoretical soil mechanics John Wiley and sons, inc., New York

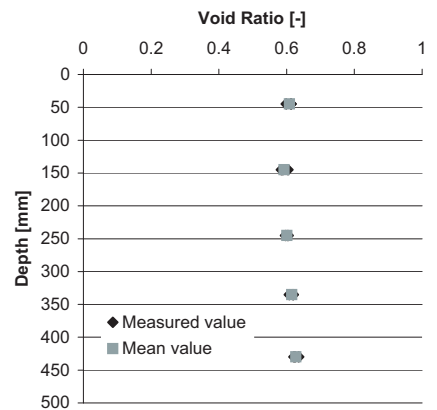
7 Appendix I: Results from tests.

The results from the performed CPT's with Aalborg University Sand No.0 are presented in this appendix.

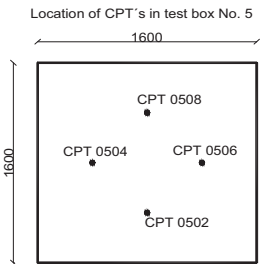
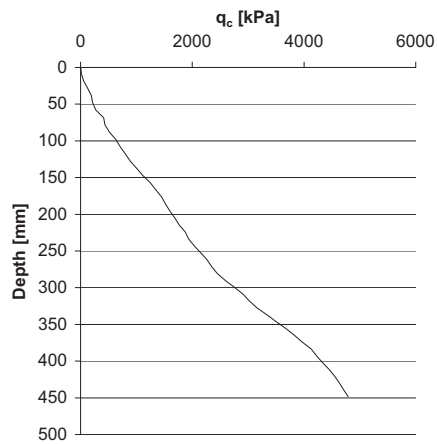
The method of compactness is given in the table at the top of each data sheet.

The measured void ratios in different depths are presented, and the results from the tests with the laboratory CPT-probe, i.e. the cone resistance, q_c is shown.

Description of soil Aalborg University Soil No. 0	Date: 05.12.01	Test box used: Large test box No. 5 Test serie 1
Preparation procedure: Standard preparation procedure using rod vibrator.	Location of samples for void ratio: Samples is taken with in a radius of 200mm around the respective CPT.	

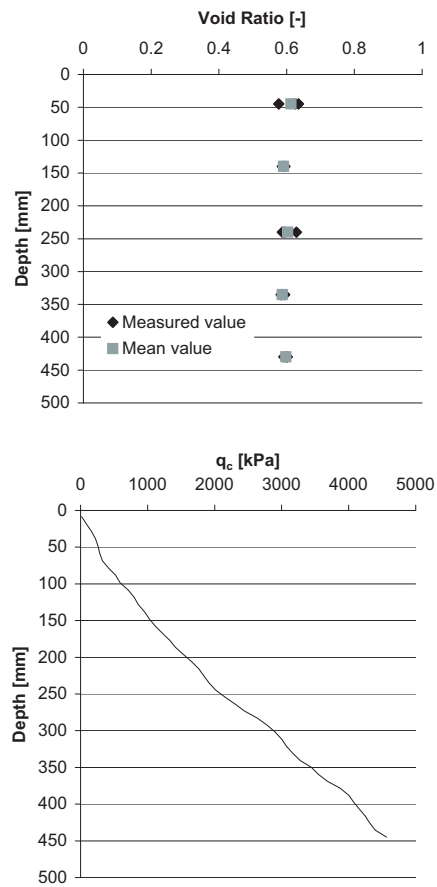


Depth [mm]	Void ratio
45	0.613
	0.613
	0.599
145	0.604
	0.589
	0.584
245	0.605
	0.596
	0.602
335	0.618
	0.62
	0.608
430	0.636
	0.621
	0.625

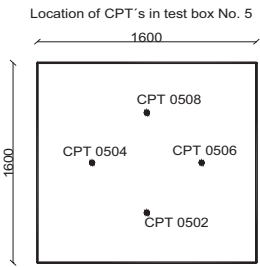


Job: Laboratory CPT-test		Remarks: 4 set of experiments is performed in this test box.
Exc: KAL	Eval: KAL	

Description of soil Aalborg University Soil No. 0	Date: 05.12.01	Test box used: Large test box No. 5 Test serie 2
Preparation procedure: Standard preparation procedure using rod vibrator.	Location of samples for void ratio: Samples is taken with in a radius of 200mm around the respective CPT.	

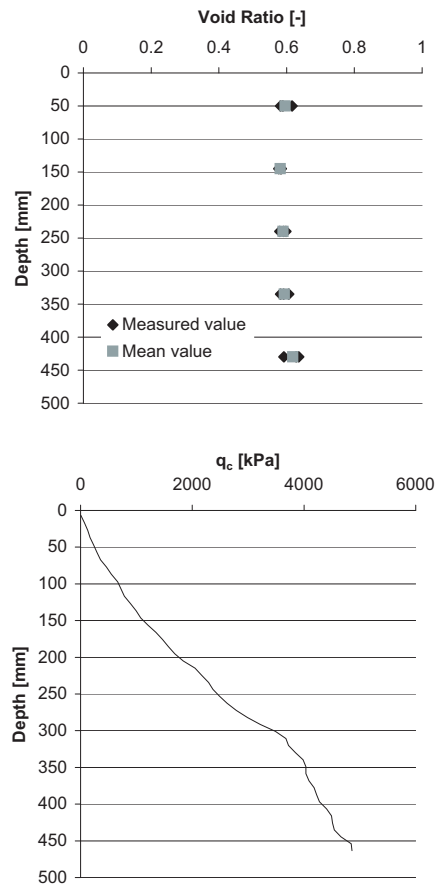


Depth [mm]	Void ratio
45	0.577
	0.635
	0.626
140	0.595
	0.587
240	0.594
	0.587
	0.629
335	0.584
	0.584
	0.594
430	0.602
	0.6
	0.592

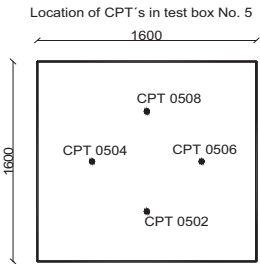


Job: Laboratory CPT-test		Remarks: 4 set of experiments is performed in this test box.
Exc: KAL	Eval: KAL	

Description of soil Aalborg University Soil No. 0	Date: 05.12.01	Test box used: Large test box No. 5 Test serie 3
Preperation procedure: Standard preperation procedure using rod vibrator.	Location of samples for void ratio: Samples is taken with in a radius of 200mm around the respective CPT.	

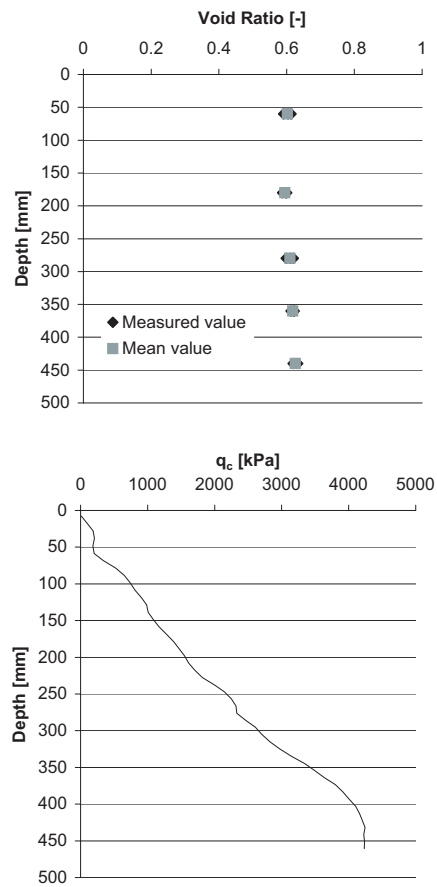


Depth [mm]	Void ratio
50	0.589
	0.582
	0.616
145	0.577
	0.584
	0.582
240	0.598
	0.58
	0.591
335	0.606
	0.582
	0.591
430	0.628
	0.592
	0.636

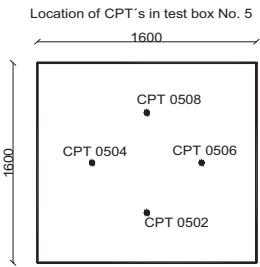


Job: Laboratory CPT-test		Remarks: 4 set of experiments is performed in this test box.
Exc: KAL	Eval: KAL	

Description of soil Aalborg University Soil No. 0	Date: 05.12.01	Test box used: Large test box No. 5 Test serie 4
Preperation procedure: Standard preperation procedure using rod vibrator.	Location of samples for void ratio: Samples is taken with in a radius of 200mm around the respective CPT.	

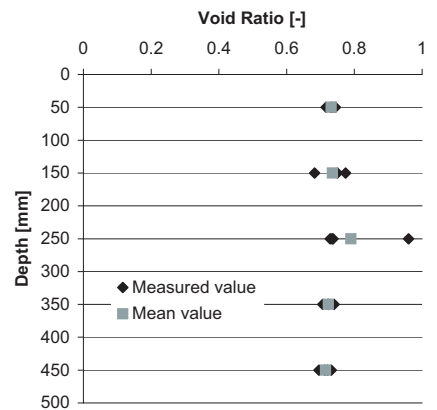


Depth [mm]	Void ratio
60	0.604
	0.613
	0.591
180	0.588
	0.6
	0.597
280	0.599
	0.62
	0.611
360	0.613
	0.622
	0.621
440	0.633
	0.619

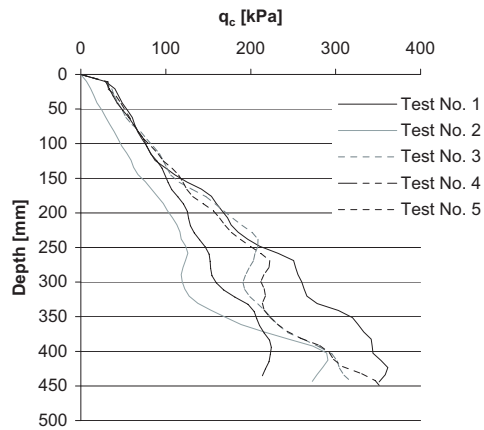


Job: Laboratory CPT-test		Remarks: 4 set of experiments is performed in this test box.
Exc: KAL	Eval: KAL	

Description of soil Aalborg University Soil No. 0	Date: 11.10.01	Test box used: Calibration container No. 2
Preperation procedure: Water pluviation		

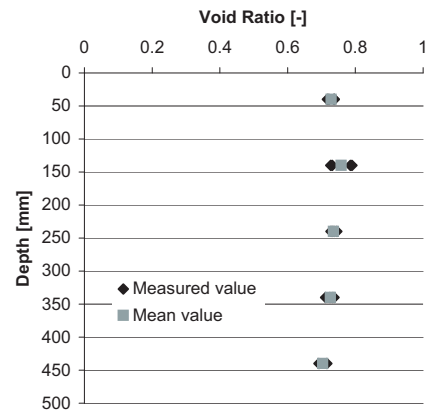


Depth [mm]	Void ratio
50	0.7168
150	0.7355
250	0.7436
350	0.7496
450	0.774
	0.6827
250	0.96
	0.7283
	0.7339
	0.737
350	0.74
	0.707
	0.7224
	0.7229
450	0.6952
	0.7208
	0.7124
	0.7316

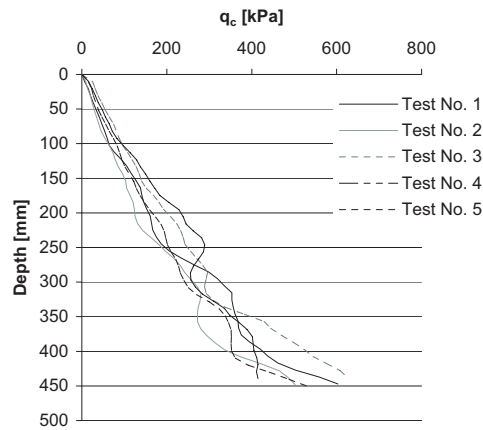


Job: Laboratory CPT-test		Remarks: One of the CPT's show a considerable lower resistance then the rest.
Exc: KAL	Eval: KAL	

Description of soil Aalborg University Soil No. 0	Date: 17.10.01	Test box used: Calibration container No. 3
Preperation procedure: Water pluviation followed by 2x1 sec ext vibration (wood between) 1/3 down at 5 pos.		

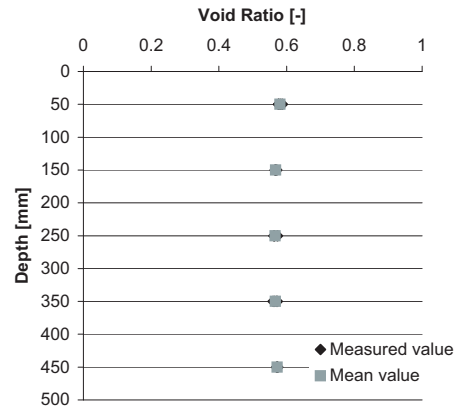


Depth [mm]	Void ratio
40	0.722
	0.717
	0.737
	0.738
140	0.785
	0.727
	0.79
	0.732
240	0.732
	0.737
	0.728
	0.745
340	0.732
	0.737
	0.725
	0.712
440	0.692
	0.716

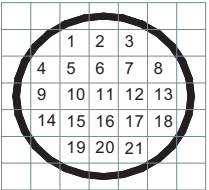
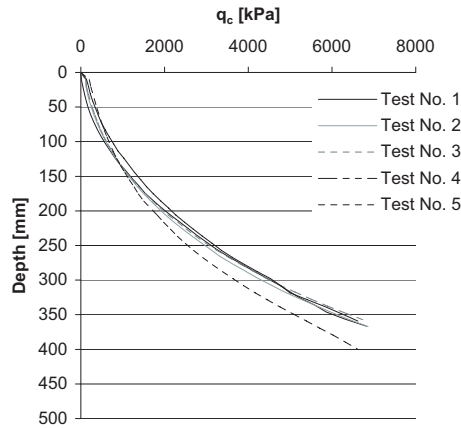


Job: Laboratory CPT-test		Remarks: No clear influence of external vibration.
Exc: KAL	Eval: KAL	

Description of soil Aalborg University Soil No. 0	Date: 22.10.01	Test box used: Calibration container No. 4
Preperation procedure: Water pluviation followed by two times vibration with rod vibrator of all squares.		

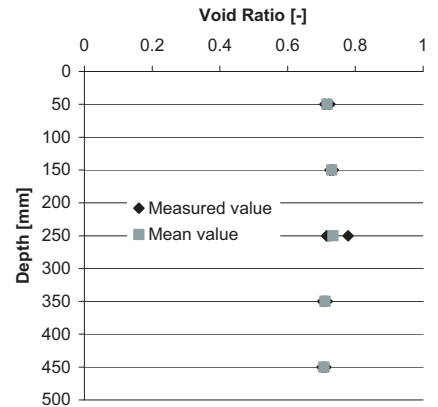


Depth [mm]	Void ratio
50	0.576
	0.582
	0.587
	0.577
150	0.566
	0.567
	0.571
250	0.562
	0.573
	0.564
350	0.571
	0.56
	0.565
	0.572
450	0.572
	0.574
	0.571
	0.572

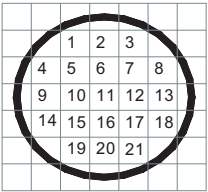
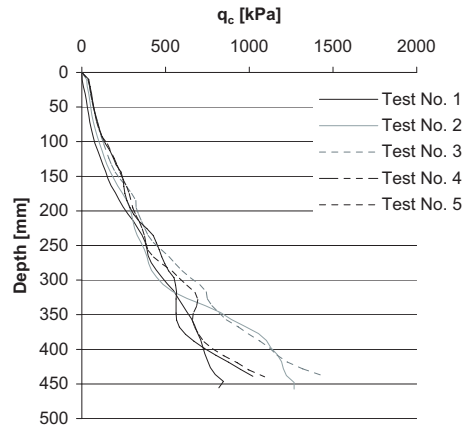


Job: Laboratory CPT-test		Remarks:
Exc: KAL	Eval: KAL	

Description of soil Aalborg University Soil No. 0	Date: 25.10.01	Test box used: Calibration container No. 5
Preparation procedure: Water pluviation followed by 3x3 sec ext. vibration (directly on chamber) 1/3 down at 6 pos.	Location of CPT: 11, 13, 20, 9, 2	Location of sample for void ratio: 5, 7, 15, 17

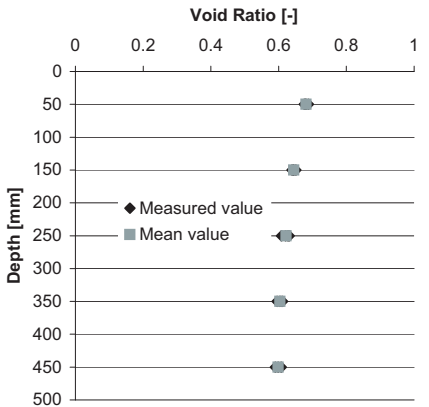


Depth [mm]	Void ratio
50	0.7095 0.7248 0.7212 0.7113
150	0.7255 0.7338 0.7258 0.7348
250	0.7173 0.7244 0.7788 0.7151
350	0.7114 0.7037 0.7095 0.716233
450	0.7124 0.7082 0.7017

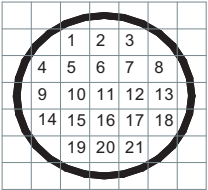
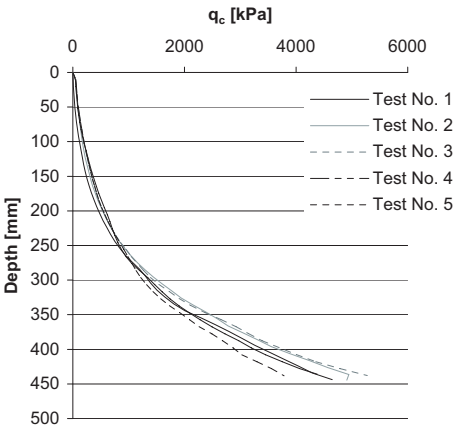


Job: Laboratory CPT-test		Remarks:
Exc: KAL	Eval: KAL	

Description of soil Aalborg University Soil No. 0	Date: 07.11.01	Test box used: Calibration container No. 6
Preparation procedure: Two times vibration in: 5, 7, 15, 17	Location of CPT: 20, 13, 2, 9, 11	Location of sample for void ratio: 6, 10, 12, 16

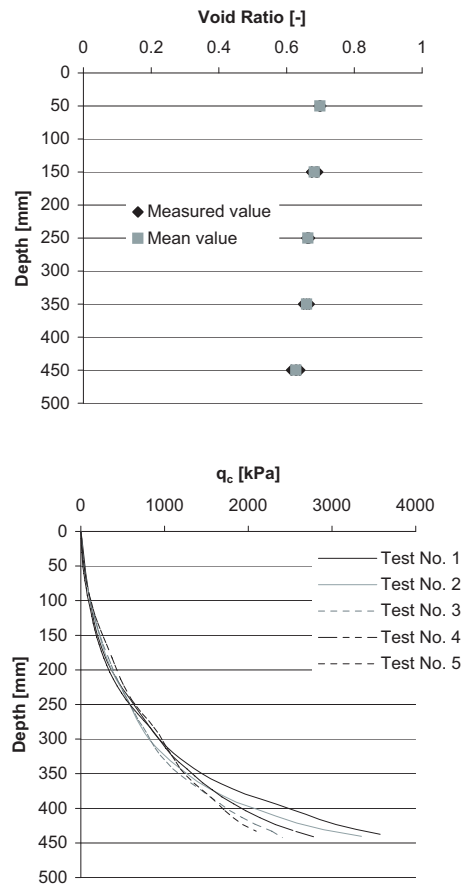


Depth [mm]	Void ratio
50	0.680788 0.678619 0.676053 0.688034
150	0.643287 0.644978 0.650816 0.639566
250	0.627363 0.608602 0.630925 0.620182
350	0.602991 0.611609 0.595261 0.606582
450	0.590269 0.598584 0.607827

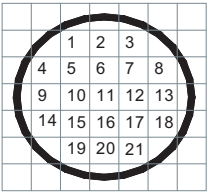


Job: Laboratory CPT-test		Remarks: The void ratio is decreasing with the depth. CPT-test No.5 is close to a vibration hole.
Exc: KAL	Eval: KAL	

Description of soil Aalborg University Soil No. 0	Date: 15.11.01	Test box used: Calibration container No. 7
Preparation procedure: One time vibration in: 5, 7, 15, 17	Location of CPT: 20, 13, 2, 9, 11	Location of sample for void ratio: 6, 10, 12, 16



Depth [mm]	Void ratio
50	0.695793
	0.698946
	0.698495
	0.70098
150	0.674371
	0.686996
	0.674006
	0.691345
250	0.659634
	0.66269
	0.667314
	0.662618
350	0.649965
	0.659239
	0.666988
450	0.629263
	0.638971
	0.614321
	0.626569



Job: Laboratory CPT-test		Remarks: The void ratio is decreasing with the depth.
Exc: KAL	Eval: KAL	